

Multipath Fading in Mobile Communication Systems

Sachin S (EE16B037), Dhanush Krishna (EE16B009) and Vishnu Beji (EE16B044)

Abstract—A signal can travel from transmitter to receiver over multiple reflective paths, this phenomenon is referred to as multipath propagation. It causes attenuation, phase distortion and inter-symbol interference all of these effects together is termed under 'multipath fading'. This paper is aimed at manifesting various fading techniques (long term fading, short term fading etc) both through simulations and through practical measurements.

I. INTRODUCTION

Multipath fading can cause fluctuations in the received signals amplitude, phase, and angle of arrival. There are two main manifestations of a fading channel namely large scale fading and small scale fading. Large scale fading involves computing the mean path loss (nth-power law) and a log normally distributed variation about the mean. Small scale fading is when signal takes a relatively shorter path. In Small Scale fading it can be seen that the effect of various paths taken by the signal to reach the destination can be modelled as a 'Rayleigh pdf' (or a 'Rician pdf' in special cases).

II. RAYLEIGH FADING

Rayleigh fading is the form of fading often experienced in an environment where there is a large number of reflections present. No single path that dominates i.e., LOS(Line of Sight) and statistical approach is required. Rayleigh fading is a statistical model for the effect of a propagation of radio signals in such an environment. If there is a dominant line of sight, Rician fading may be more applicable. Cellular telephones being used in a dense urban environment fall into this category. If there is no dominant component to the scatter, then such a process will have zero mean and phase evenly distributed between 0 and 2π radians. We model the envelope by Rayleigh pdf.

The envelope of the channel response is modeled to have a Rayleigh distribution and the probability density function for this is,

$$p_R(r) = \frac{2r}{\Omega} e^{-r^2/\Omega}$$

where $\Omega = E(R^2)$

III. LARGE SCALE FADING

We will be understanding the concepts behind large scale fading, such as shadowing, and how to calculate the mean path loss and variation about mean. Simulations for this will be done through MATLAB after fixing/evaluating parameters such as the reference distance (d_0), path loss exponent (n) and the standard deviation for the log-normal variation.

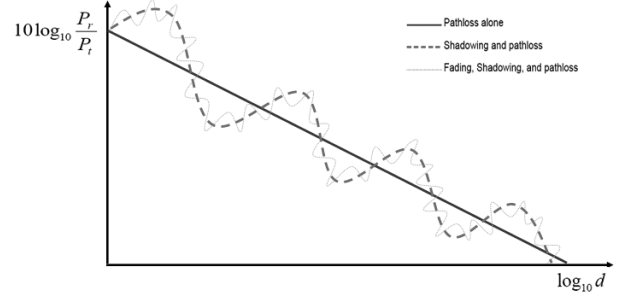


Fig. 1. A general plot of large scale fading with path loss and shadowing

A. Heat Map of Received Signal

We collected the received powers at different spots along the main corridors in IIT Madras campus. The heat map of received signals corresponds to Vodafone 4G LTE cellular network. The map observes an area under the range of multiple transmission towers as is evident from various peaks and troughs in the path. A key observation is how the fading intensifies in areas shadowed extensively by trees. The readings are based on geo-coordinate and signal strength data abstracted from "Cell Signal Monitor" application that made discrete measurements every 5 seconds. About 4000 data points are being taken into account.



Fig. 2. Heat Map of Received Signals in IIT Campus

B. Observations

Here is a plot of the signal power in dBm with respect to distance from the transmitter(measured in our hostel). The readings are taken very close to a transmitter tower and measurement is from the ground. The region to the right of the red area receives line of sight path and hence follows

usual path loss with distance. The region to the left does not involve line of sight and is blocked by the building supporting the tower. The exact shadowing property of the building is unclear but the increase in number of floors blocking LOS gives lesser signal strength near receiver.

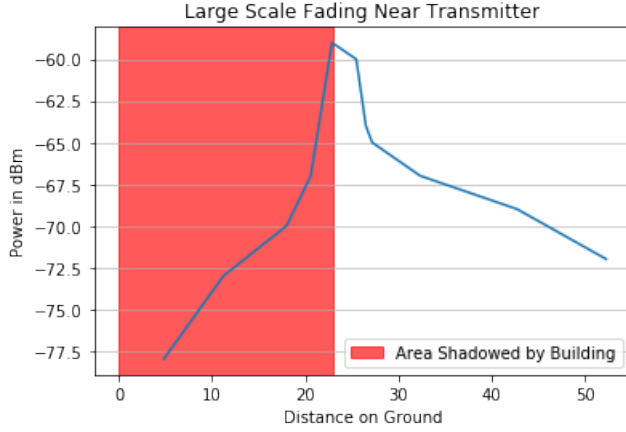


Fig. 3. Shadowing and Large Scale Fading

As we try measuring larger distance variations multiple factors come into picture. In Fig. 4 we can see that there is a maximum that occurs at distance zero the signal decreases with distance. This is because the receiver was near a transmitter tower located at $d=0$. We get a minimum and then again a maximum because we went further away from one transmitter and then the receiver picked the signals from another cell tower located at $d=150\text{m}$. The green region indicates the transition from one cell to another. We also observe shadowing effects overlapping with the path loss component. The plot is consistent with this assessment as per two sets of readings.

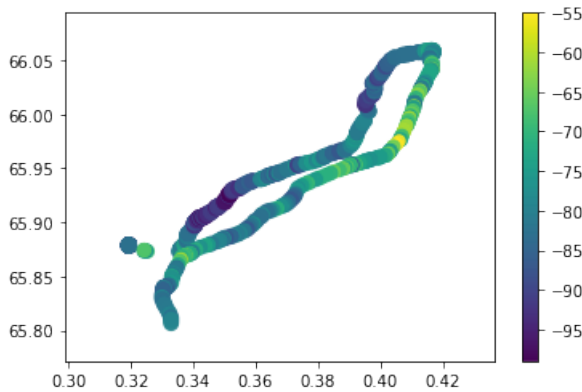


Fig. 4. 3G UMTS signal strength vs geo-coordinates

Signal strength readings at each geo-coordinate from Bonn Avenue and Delhi Avenue of IIT Madras for 3G UMTS and 4G LTE networks, given in figures 4 and 5 respectively show how the corresponding strengths are from different sets of base stations. In the top-right corner of geo-coordinates, the

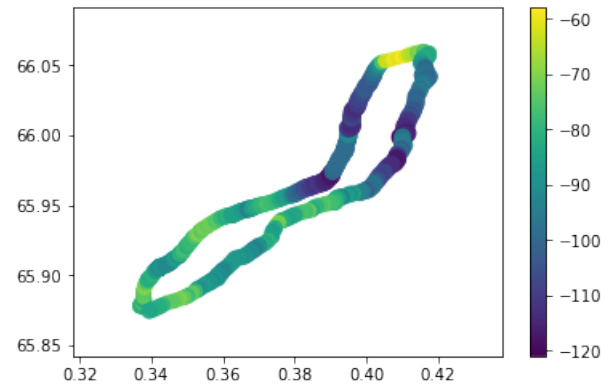


Fig. 5. 4G LTE signal strength vs geo-coordinates

signal is high for 4G LTE due to proximity of its tower and less shadowing while 3G UMTS has a near blind spot as it's 3G tower is far off.

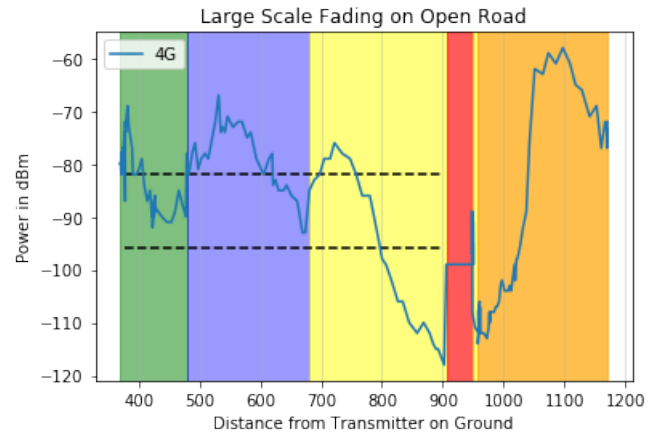


Fig. 6. Handoff between cells

Fig. 6 shows how signal variations occur at different regions and when the hand-off is initiated. Each colour corresponds to a particular cell ID. The dotted lines are a band from -82dBm to -95dBm which is where 4G LTE initiates hand-off. Below -99dBm 4G fails to work. Interesting we notice that in the yellow region the strength goes way below -99dBm before initiating hand-off. This is because of a 4G network blind spot in the area. The red region is 3G network and the cell network only switches to it under sufficient lack of 4G network. Even though the signal strength is of the range -110dBm a hand-off is initiated back to 4G. From this it is clear how cell switching is not just mere based on signal strength. Another interesting observation in this plot is how there is a spike in strength after hand-off. The mobile phone does not instantly switch to another available network but takes a relaxation width until when to decide the switching. This avoids unnecessary and chaotic switching between cells.

C. Simulating the path loss

In python we have simulated the signal strength at a distance from the tower. It comes with regular path loss over

distance as well as added rayleigh noise to get closer to practical scenario. The parameters used for this simulation are:

The Transmitter Power just outside far field: -69.77dBm ,
 Height of Base Station: 50m ,
 Height of Receiver: 5m ,
 Frequency: 860MHz ,
 Directional Gain Base Station: 1000,
 Directional Gain Mobile: 100.

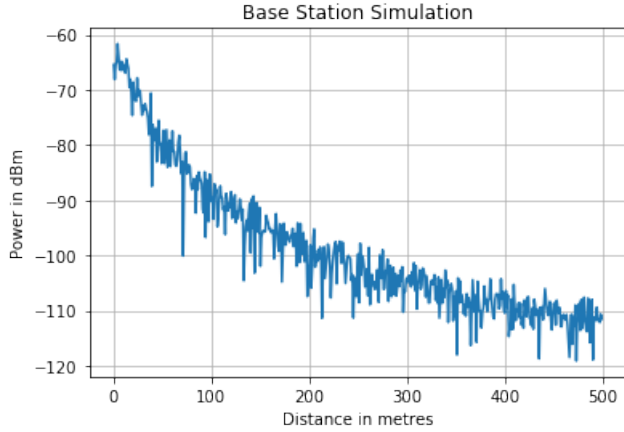


Fig. 7. Large scale fading simulation

Subsequently, the one dimensional path loss was extrapolated to create signal strength pattern around a base station on a two dimensional area on the ground, and we have obtained the surface plot in Fig. 8. The noise here is uncorrelated with the radial and angular displacement from the tower.

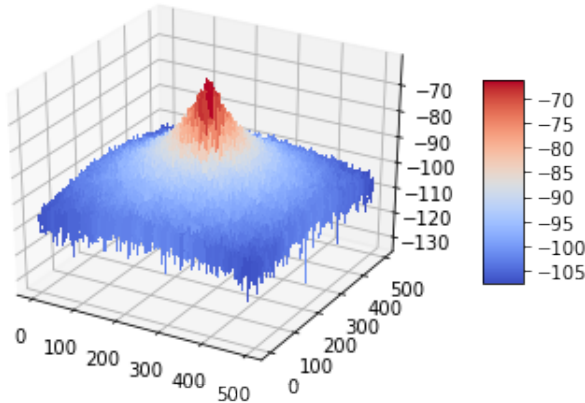


Fig. 8. Signal Strength on the ground around base station

The same single base station scenario in contour plot gives us Fig. 9. We then looked at multiple base stations to see how they interact and obtain the most effective type of pattern for mobile communication. As a finite number of towers can only give rise to polygonal arrangements we proceed optimizing in this regime. For a given distance between cell and boundary, maximum area is covered by hexagonal arrangement in comparison with triangular/square patterns.

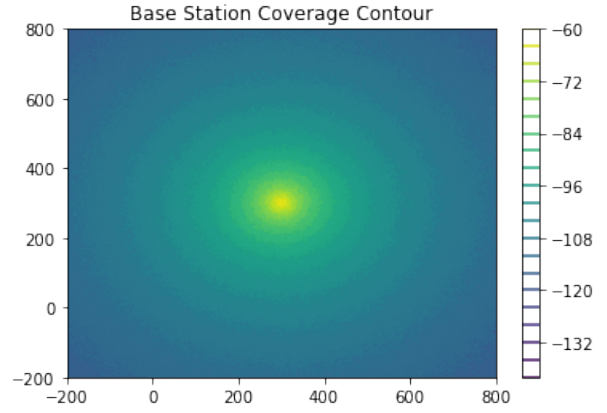


Fig. 9. Single Base Station Contour Plot

Fig. 10 shows the network strength patterns picked by a mobile moving arbitrarily on the 2D plane. The hand-off here is defined by maximas of signal strengths as we are taking identical towers with zero shadowing.

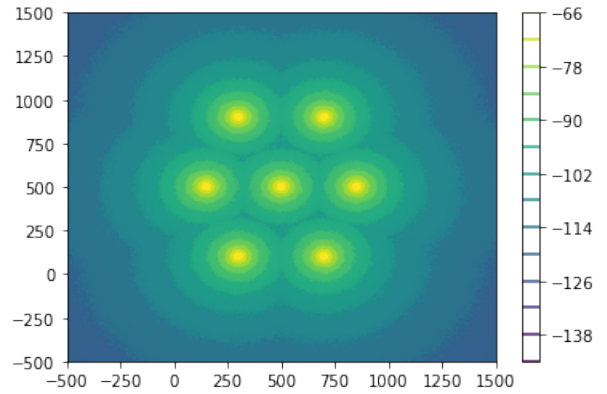


Fig. 10. Hexagon Base Station Network Contour Plot

For practical purposes this hexagonal arrangement alone will not suffice. Therefore we do a technique called cell splitting where we essentially split the network coverage area under a cell into a few smaller cells wherever there are chances of reduction in strength. The additional base stations will be smaller in height and transmitted power. Fig. 11 shows such an arrangement. In all the above cases we are assuming omni-directional antennas.

IV. SMALL SCALE FADING

This section will focus on understanding small scale fading due to time spread and time variance in both time and frequency domains. Effects like flat fading and frequency selective fading due to time spread and Doppler Spread due to time variance will be discussed. Classification of small scale fading is given in the below image Fig. 12:

A. Frequency Selective Fading

When the bandwidth (equal to the sampling rate) of the signal is large, the channel fails to provide the same

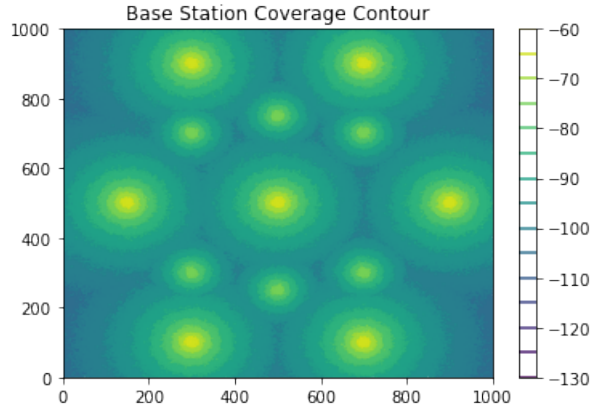


Fig. 11. Interlinked Base Station Network Contour Plot

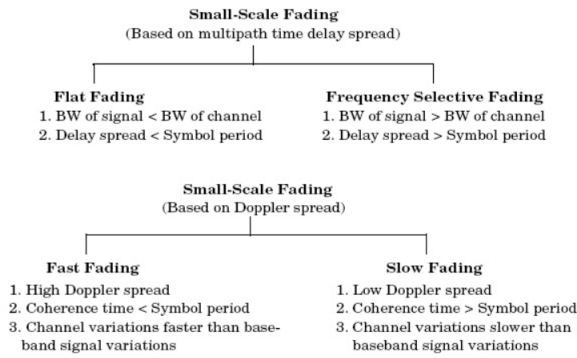


Fig. 12. Small Scale Fading Classification

gain for all the frequencies present in the signal. Different frequency components of the signal therefore experience different fading. In other words the minimum sampling frequency required is so high that there is not enough time for all the multipath components to arrive before the next sampling event. The received multipath components of a symbol extend beyond the symbol's time duration. This causes frequency selective fading and induces ISI (channel-induced ISI).

In our simulation, we have chosen the delay spread to be $1.5\mu s$ for 4 multipath components with varying gains, the signal bandwidth as $5MHz$ which in the case of QPSK Modulation corresponds to $2500k$ symbols per second, this gives us a symbol period of $0.4\mu s$ which is less than the delay spread.

In Fig. 13 we can see that multipath components (4 components) of the symbol extends to other symbols as well, justified further in Fig. 14 is that the bandwidth of the signal is just too big for the channel to give a constant gain.

In Fig. 15, we see that the 500 QPSK modulated symbols sent is not at all concentrated around their 4 empirical values (marked by red crosses).

B. Flat Fading

In flat fading, the bandwidth of the signal is sufficiently small so that the channel remains roughly flat for all the

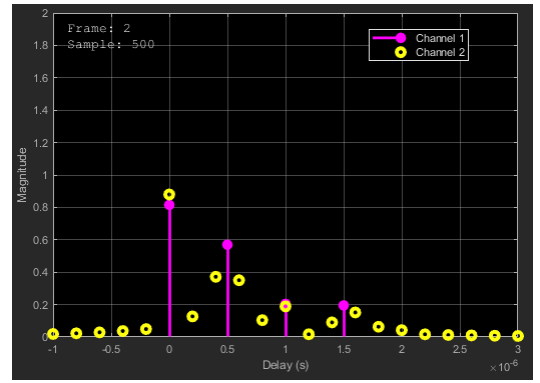


Fig. 13. Frequency Selective Fading (Time Domain)

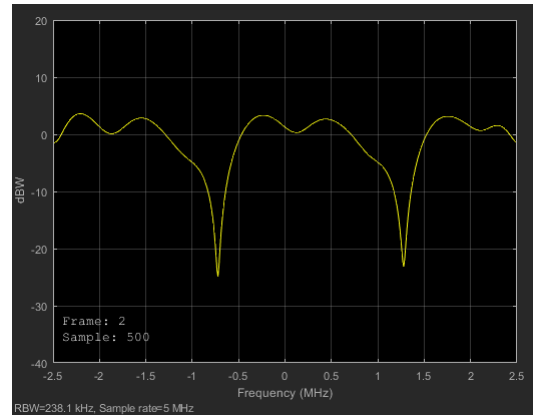


Fig. 14. Frequency Selective Fading (Frequency Domain)

frequencies present. Therefore, all frequency components of the signal will experience the same magnitude of fading. The delay spread is less than the symbol period.

In our simulation, we have chosen the delay spread to be $1.5\mu s$, the signal bandwidth as $200kHz$ which in the case of QPSK Modulation gives $100k$ symbols per second. This gives the symbol period to be $10\mu s$ which is more than the delay spread.

It can be observed in Fig. 16 that by decreasing the bandwidth we effectively received all faded components within a sample period. Frequency spectrum is flat as expected. Fig. 18 shows that the transmitted symbols are fairly concentrated around the empirical QPSK symbols.

C. BER analysis of the Rayleigh channel for QPSK

From plots in Fig. 15 and Fig. 18, we can say that the received symbols were definitely more accurate and closer to the expected values in the case of flat fading in Fig. 18. However it still suffers from some level of spreading around empirical values due to the fading nature of the channel. This can be understood better from the simulated plot in Fig. 19 showing the BER values for various SNRs. It can be seen that the BER values for frequency selective fading is the highest, next only to the BER values for flat fading, consistent with the previous simulations in figures 15 and 18.

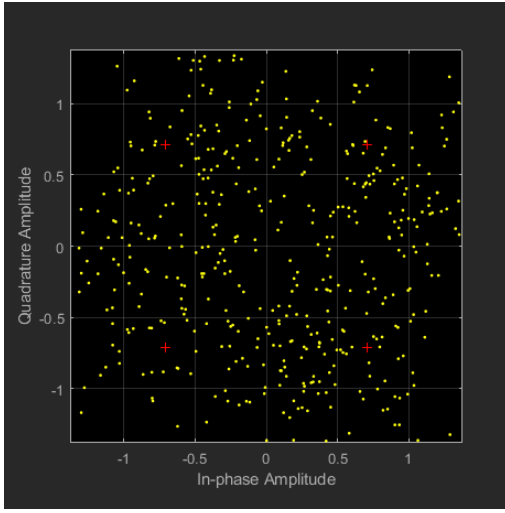


Fig. 15. Signal constellation (time dispersed QPSK)

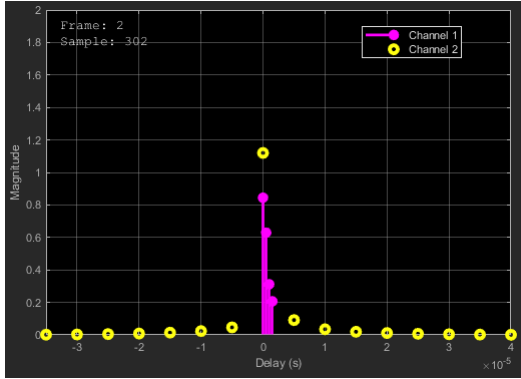


Fig. 16. Flat Fading (Time Domain)

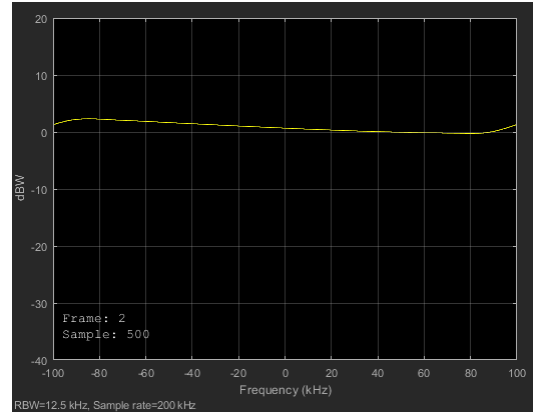


Fig. 17. Flat Fading (Frequency Domain)

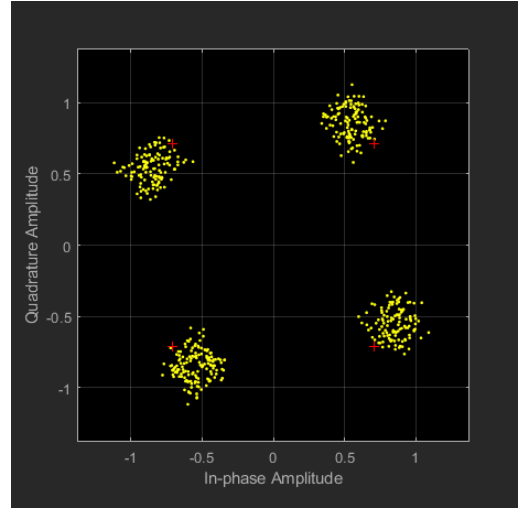


Fig. 18. Signal constellation (time dispersed QPSK)

D. Doppler Shift

A completely analogous characterization of the time-variant nature of the channel can begin in the Doppler shift (frequency) domain. Fig. 20 shows a Doppler power spectral density $S(\nu)$, plotted as a function of Doppler-frequency shift ν (Hz). The sharpness and steepness of the boundaries of the Doppler spectrum are due to the sharp upper limit on the Doppler shift produced by a vehicular antenna traveling among the stationary scatterers of the dense scatterer model. The largest magnitude (infinite) of $S(\nu)$ occurs when the scatterer is directly ahead of the moving antenna platform or directly behind it.

The simulation parameters considered for the doppler spread analysis are as follows. The carrier frequency of transmission was set at 2GHz and for a receiver travelling at a speed of $5m/s$ we get a frequency shift (f_d) of 20Hz according the equation

$$f_d = \frac{v}{\lambda}$$

where λ is the wavelength of the signal and v is the velocity of the receiver.

The channel was simulated for 10000 bits and about 5000

iterations were averaged out to get a smooth plot resembling the empirical curve. Fig. 20 shows peaks around 20Hz from the central frequency on each side which is consistent with our calculations before.

V. RAYLEIGH FADING OBSERVATIONS

Small scale fading in non-LOS paths is usually a result random variations in amplitude and phase due to multipath and other environmental factors. It can be modelled statistically through Rayleigh distribution. The received power fluctuates in the following way:

For the ICSR Auditorium, IIT Madras, we attempted characterizing received signal variations while receiver is stationary. The 4G LTE network operates at 1.8GHz which amounts to $\lambda = 16.6cm$. For small movements close to λ distance the fading involves multipath effect. This is primarily random and signal strength can be modelled as a random variable with Rayleigh distribution. From about 232 non-null observations we obtain the histogram of received signals. This nearly follows Rayleigh pdf (Fig. 23). Fig. 22 shows, a lot of variance is observed due to multipath fading indicating further randomness due to multiple reflected paths

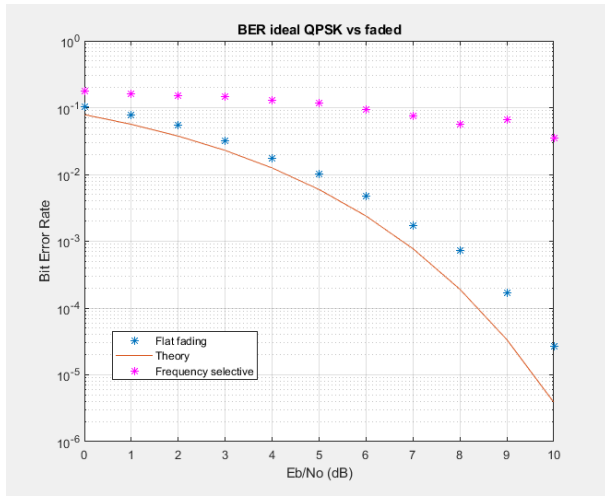


Fig. 19. Signal constellation (time dispersed QPSK)

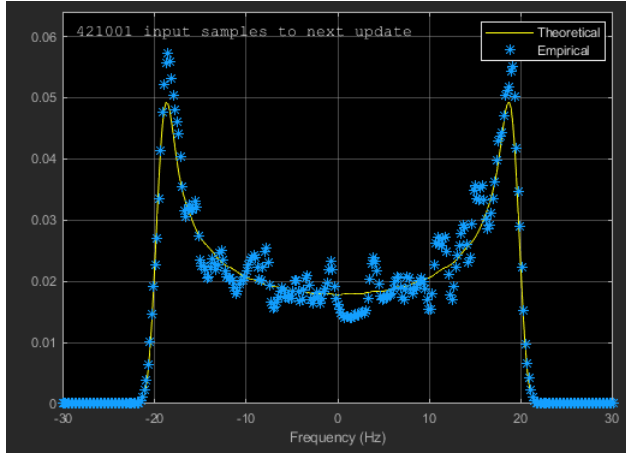


Fig. 20. Doppler power spectrum

in the hall. The amount of deep fades and peaks are less whereas maximum of our observations lie around the mean = -89.14 dBm.

VI. SIMULATING MULTIPATH FADING

We used the Rayleigh Channel Module in MATLAB to simulate these processes and explored how the module calculates the values required. The Communications Toolbox use the band-limited discrete multipath channel model. The multipath fading channel is modeled as a linear finite impulse-response (FIR) filter. The set of samples at the input are s_i and samples at output are y_i . They are related as,

$$y_i = \sum_{n=-N_1}^{N_2} s_{i-n} g_n$$

where g_n is the set of tap weights given by

$$g_n = \sum_{k=1}^K a_k \text{sinc} \left[\frac{\tau_k}{T_s} - n \right], -N_1 \leq n \leq N_2$$

where T_s is the input sample period,

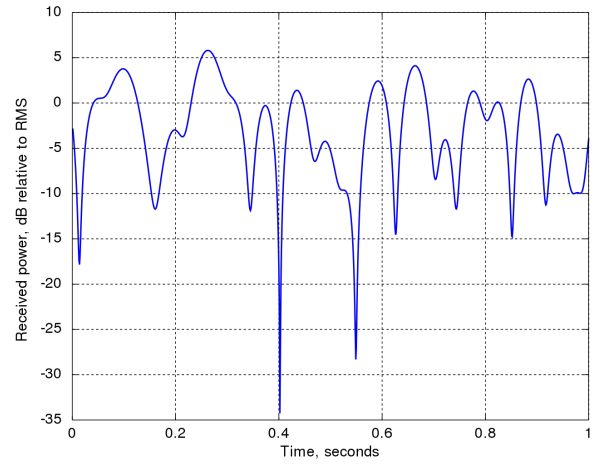


Fig. 21. Signal received for a stationary receiver

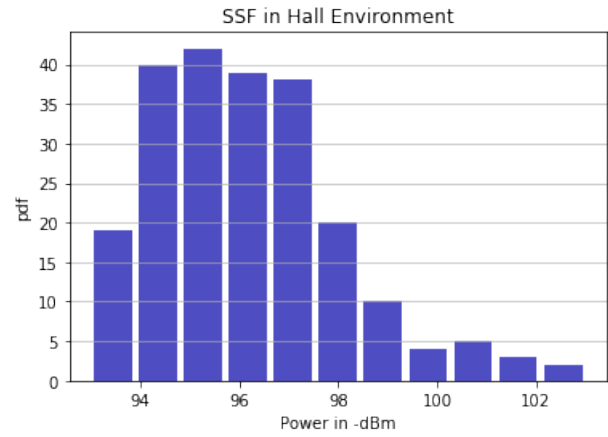


Fig. 22. Observed small scale variations at ICSR Auditorium, IIT Madras

τ_k is the set of path delays, a_k is the set of complex path gains which are uncorrelated with each other and N_1 and N_2 are chosen such that $|g_n|$ is small when n is beyond the limits. To generate the complex path gains, the toolbox uses two techniques, filtered Gaussian noise and Sum-of-Sinusoids technique.

VII. OFDM METHOD

We also explored what the later versions of mobile networks used to reduce multipath fading. Introduced to provide digital modulation scheme to reduce Inter Symbol Interference (ISI) and Inter Channel Interference (ICI). OFDM is resilient to frequency selective fading and has high spectral efficiency but sensitive to time selective fading due to Doppler spread. In OFDM, the available bandwidth is subdivided into multiple frequencies sub-carriers which overlap in frequency. Orthogonality must be maintained between sub-carriers. The sum of information signals in the discrete time domain as defined by,

$$x(k) = \frac{1}{N} \sum_{m=0}^{N-1} x^m e^{j2\pi km/N}$$

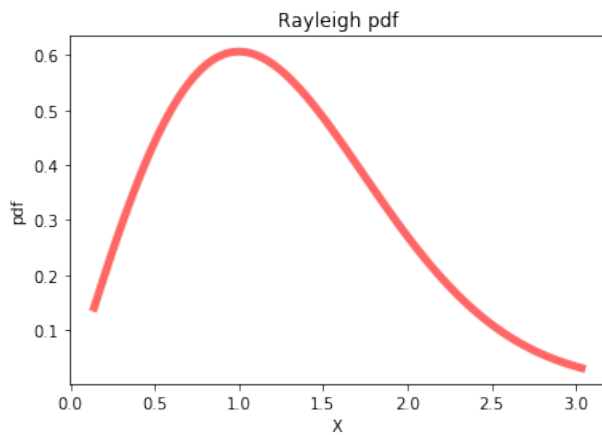


Fig. 23. Theoretical Rayleigh distribution

A wideband frequency selective channel is converted into a set of parallel flat fading narrowband channels. OFDM is the modulation of choice in 4G Long Term Evolution(LTE). Cyclic prefix(CP) contributed significantly to the process of eliminating ISI. A fraction of the OFDM Symbol is extracted from the end and is appended at the beginning. This fraction is known as Cyclic Prefix or Cyclic Extension(CE). Addition of CP results in circular convolution rather than linear convolution. CP reduces spectral efficiency but improvement in ISI adequately compensates for this reduction.

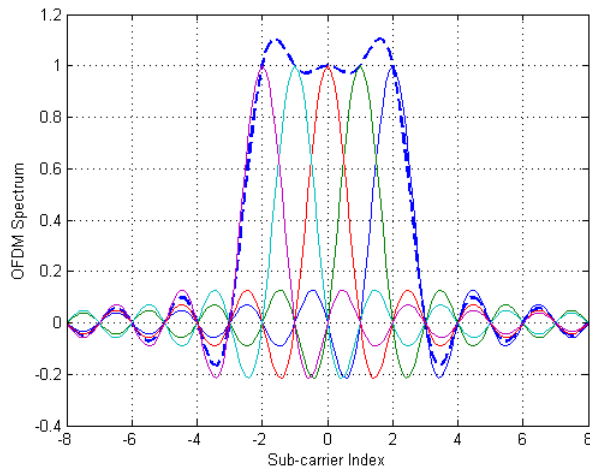


Fig. 24. OFDM Spectrum

VIII. CONCLUSION

Large-scale fading effects in real life environments can be more complex considering multiple transmitters placed unevenly across the ground. The variations still capture the effects of path loss and shadowing to a great extent. Considering small scale fading effects, the randomness of received signal follows a distribution very similar that of Rayleigh pdf. Yet further accuracies can be obtained by taking higher numbers of measurements in low power condition

where we may observe more deep fades. The empirical and theoretical values in various simulation with regard to flat fading, frequency selective fading and doppler shifts also seem to match.

The practical measurements obtained and analyzed along with general realistic models considered for each variant in simulations helped in understanding of multipath fading and its variations in depth. The understanding of MATLAB Rayleigh object [8] working further develops insight into modelling Rayleigh fading in a realistic manner.

REFERENCES

The following are the links to the websites and documents/papers we have utilized:

- [1]https://en.wikipedia.org/wiki/Rayleigh_fading
- [2]<https://www.electronics-notes.com/articles/antennas-propagation/propagation-overview/multipath-fading.php>
- [3]<https://ocw.mit.edu/courses/electrical-engineering-and-computer-science/6-450-principles-of-digital-communications-i-fall-2006/lecture-notes/book9.pdf>
- [4]<http://www.ni.com/white-paper/14916/en/>
- [5]<https://www.testforce.com/FadingBasics.pdf>
- [6]<https://ieeexplore.ieee.org/abstract/document/601747> r
- [7]https://www.researchgate.net/figure/Pathloss-shadowing-and-fading-versus-distance_fig1268056753
- [8]Fading Channels MATLAB - <https://in.mathworks.com/>
- [9]Performance of OFDM in Time Selective Multipath Fading Channel in 4G Systems(IEEE)
- [10]<https://www.nutag.com/blog/introduction-orthogonal-frequency-division-multiplex-ofdm>